

Runaway electron drift orbits in magnetostatic perturbed fields

G. Papp 1,2), M. Drevlak 3), T. Fülöp 2), P. Helander 3) and G.I. Pokol 1)

1) Department of Nuclear Techniques, Budapest University of Technology and Economics, Association EURATOM-HAS, Budapest, Hungary

2) Nuclear Engineering, Department of Applied Physics, Chalmers University of Technology, Association EURATOM-VR, Göteborg, Sweden

3) Max-Planck-Institut für Plasmaphysik, Greifswald, Germany

e-mail contact of main author: papp@reak.bme.hu

Abstract. Disruptions in large tokamaks can lead to the generation of a relativistic runaway electron beam that may cause serious damage to the first wall. To mitigate the disruption and suppress the runaway beam the application of resonant magnetic perturbations has been suggested. In this work we investigate the effect of resonant magnetic perturbations on the confinement of runaway electrons by simulating their drift orbits in magnetostatic perturbed fields and calculating the orbit losses for various initial energies and magnetic perturbation magnitudes. In the simulations we use a TEXTOR-like configuration and solve the relativistic, gyro-averaged drift equations for the runaway electrons including synchrotron radiation and collisions. The results indicate that runaway electrons are well confined in the core of the device, but the onset time of runaway losses closer to the edge is dependent on the magnetic perturbation level and thereby can affect the maximum runaway current. However, the runaway current damping rate is not sensitive to the magnetic perturbation level, in agreement with experimental observations.

1. Introduction

A serious problem facing ITER and similar devices is the occurrence of plasma-terminating disruptions. During a disruption a very quick cooling of the plasma takes place, so that the resistivity drops and, as a result, the toroidal electric field rises dramatically. This electric field can detach a fraction of the electrons (in velocity space) from the bulk of the plasma and accelerate them to very high energies (tens of MeV). The detached electrons are normally referred to as runaway electrons [1]. The beam of runaway electrons usually drifts to the wall of the tokamak, where it can cause severe damage. Unmitigated disruptions represent a severe risk for ITER and should be avoided by reliable control of the plasma discharge. An extrapolation of the effects of a disruption from existing devices to ITER is affected by uncertainties, which should be minimized to guarantee the integrity of the machine. A good understanding and modelling capability of runaway electrons should aid in evaluating different methods aimed at mitigating their effects.

One of the most discussed disruption mitigation methods is the use of resonant magnetic perturbations (RMP). In this work we concentrate on the use of RMP to increase the runaway electron losses. This has been shown to work well in various experiments: in JT-60 it was shown that runaways were absent for a sufficient high perturbation field [2]; in TEXTOR the runaway losses were enhanced by RMP and it was shown that the runaway avalanche can be suppressed [3, 4, 5, 6]; and also in Tore-Supra applying an ergodic divertor led to enhanced losses [7]. However, recent results from JET indicate that RMP have not been successful in suppressing the runaway beam [8]. The reason for the difference in the experimental success of suppressing runaways in various devices is

not yet properly understood.

Previous theoretical work has shown that if the radial diffusion of runaway electrons is sufficiently strong, avalanches can be prevented and the magnetic perturbation level necessary for this has been estimated to $\delta B/B = 10^{-3}$ for typical tokamak parameters [9]. Due to the complexity of the effect of magnetic drift on diffusion, a reliable picture of how the runaway electrons are transported out of the plasma can only be obtained via three-dimensional numerical modelling of the runaway electron drift orbits.

2. Modelling

We solve the relativistic, gyro-averaged equations of motion for the runaway electrons including the effect of synchrotron radiation with the ANTS (plasma simulation with drift and collisionS) code [10]. This code calculates the drift motion of particles in 3D fields and takes into account collisions with background (Maxwellian) particle distributions, using a full-f Monte Carlo approach. For the purposes of this project it has been extended to include synchrotron radiation losses and a new collision operator that is valid for both low and high velocities [11]. The runaway electron drift orbits have been calculated for typical TEXTOR-like discharges, chosen to be similar to the ones where the runaways were shown to be suppressed by resonant magnetic perturbations created by dynamic ergodic divertor (DED) coils. This divertor consists of 16 helical coils at the high field side of the device. Electric currents flowing in these coils generate a perturbation field, and a sufficiently large perturbation result in an ergodization of the magnetic field lines.

In our calculations we use a TEXTOR-like post-disruption equilibrium, with major radius $R_0 = 1.8$ m, minor radius $a = 0.46$ m, toroidal magnetic field $B_t = 2.25$ T (at $R = 1.75$ m), plasma current $I_p = 320$ kA. In TEXTOR, the runaways were generated deliberately by injection of $3 \cdot 10^{21}$ Argon atoms and therefore we assume that the post-disruption density has increased to 10 times its pre-disruption value. The density, pressure, temperature and q -profile we used are $n_e = n_0(1 - 0.9s^2)^2$, with $n_0 = 3.1 \cdot 10^{20} \text{ m}^{-3}$, $T_e = T_0(1 - 1.1s^2)^2$ with $T_0 = 10$ eV and $q = q_0(1 - \beta s^2)^{-\alpha}$, with $\beta = 1 - (q_0/q_a)^{1/\alpha}$, $q_0 = 0.97$, $q_a = 4$, $\alpha = 0.8$ and s is the normalized flux. The unperturbed magnetic equilibrium has been calculated by VMEC [12] for the parameters above and the TEXTOR coils. The magnetic field perturbations are modelled to be similar to the ones produced by DED-coils on TEXTOR in the 6/2 DC operation mode [13, 14]. Figure 1a shows a sketch of this coil configuration as it is used in our simulations. The 6/2 mode in DC has

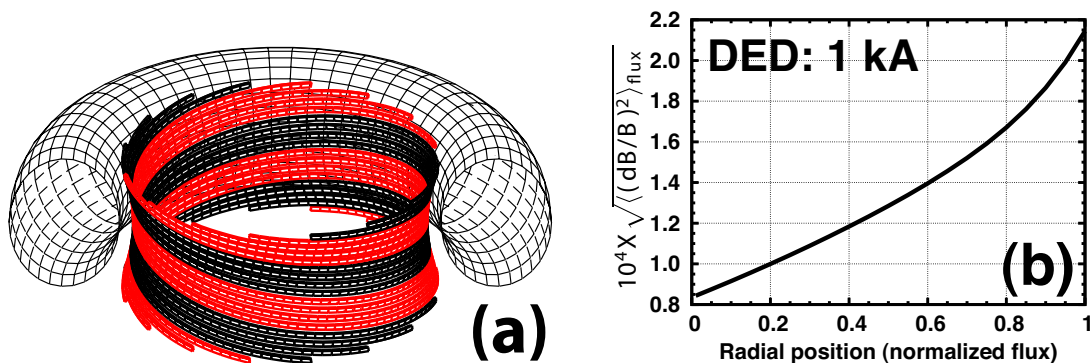


Figure 1: (a) Sketch of the two DC DED coil configurations tested in the simulation, $n = 2$. Black coils are fed with $+I_{\text{DED}}$, grey coils are fed with $-I_{\text{DED}}$. The torus marks the plasma. (b) Radial dependence of the flux surface averaged $\sqrt{\langle (\delta B/B)^2 \rangle}$ for $I_{\text{DED}} = 1$ kA.

a 180° toroidal rotation symmetry, thus the generated islands have toroidal mode number of $n = 2$. For simplicity the terminals are ignored. These coils create magnetic perturbations at the plasma periphery on the high field side of the torus that decay radially toward the inside of the plasma as shown on figure 1b. The flux-surface averaged magnetic perturbation level that is predicted to be necessary for runaway suppression $\delta B/B = 10^{-3}$ [9] corresponds to $I_{\text{DED}} = 6.7$ kA at the flux-surface $s = 0.7$ in the $6/2$ mode. This is close to the technically achievable upper limit of 7.5 kA on TEXTOR in this mode.

In the simulations we neglect the effect of shielding of magnetic field perturbations by plasma response currents. This is motivated by the fact that the shielding is expected to be small in cold post-disruption plasmas. Estimates of the plasma shielding of RMP in non-disruptive DIII-D plasmas have shown that the plasma response currents significantly reduce the effect of the perturbation field on the magnetic configuration in the core plasma [15], however we are lacking a comprehensive calculation of the shielding in disruptive plasmas. Analysis of the shielding effect is beyond the scope of the present paper, but it is clear that it would reduce the runaway losses and therefore our results will have to be interpreted as an upper limit on actual losses. In this work it is assumed that the field generated by the DED coils is significantly smaller than that from the toroidal field coils and the plasma current. Therefore, and because we neglect plasma shielding, we approximate the perturbed magnetic field by simply superimposing the field from the DED coils on the field of the unperturbed VMEC solution. The magnetic flux surfaces in the perturbed equilibrium are shown in figure 2 for $I_{\text{DED}} = 6$ kA. As the magnetic perturbation grows magnetic islands appear, the locations of which are correlated with rational values of the safety factor, and the edge region becomes ergodic. Particles outside the last intact magnetic surface leave the plasma rapidly, as will be shown later.

3. Particle radial distributions and energies

The shrinkage of the confinement zone plays an important role at high particle energies regardless of the DED. Figure 3 shows the Poincaré plots of the particle orbits with energies 1 MeV, 10 MeV and 30 MeV. One particle was launched at each radial position and followed for $t = 30$ ms simulation time. The effective boundary of the confinement volume for low energy ($E \lesssim 1$ MeV) particles coincides with the equilibrium LCFS marked with the red line as shown on figure 3a. The confinement volume shrinks with increasing particle energy. The orbits (in the unperturbed field) of the particles are circles that are displaced horizontally with respect to the flux surfaces, with a displacement that is proportional to the energy (for relativistic particles). This is the reason why the confinement region shrinks when the energy is large enough: particles outside the confinement region follow drift orbits that intersect vessel components and are lost very rapidly. The losses therefore increase with increasing particle energy. The effect of the DED on particle orbits decreases with increasing particle energy.

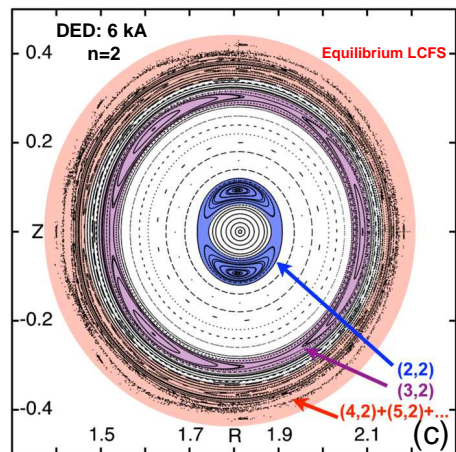


Figure 2: *Magnetic flux surfaces in a perturbed TEXTOR-like equilibrium for $I_{\text{DED}} = 6$ kA. The regions with magnetic islands are highlighted and the corresponding mode numbers are given.*

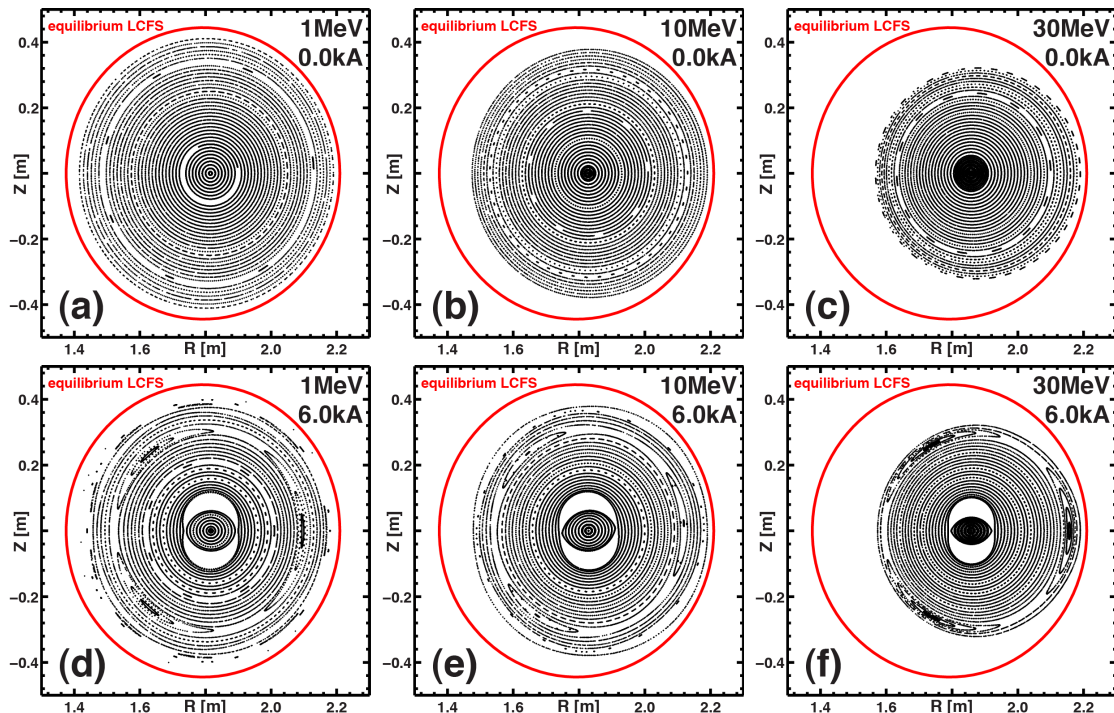


Figure 3: Poincaré plots of the particle orbits for different runaway energies and DED currents. Left to right: 1, 10 and 30 MeV; top: $I_{\text{DED}} = 0$ kA, bottom: $I_{\text{DED}} = 6$ kA.

We now turn to the examination of particle positions as functions of time. In figure 4 we have plotted the radial positions of 100 electrons with initial energy of 1 MeV, launched at the flux-surface $s = 0.7$. Runaways always travel in the direction opposite to the plasma current. In TEXTOR this is in the direction of the magnetic field, so that runaways in TEXTOR are co-passing with respect to the magnetic field. Here we study both co- and counter-passing electrons, by simply reversing their launch direction to investigate possible differences and gain insights into the physics. This reversal is not likely to occur in practice.

The particles are well confined and do not drift radially in the absence of collisions. If collisions are switched on, a slightly asymmetric radial displacement of the orbits arises, as shown in figure 4. The time instant when this happens is when particles are converted (by collisions) from passing to trapped. This gives rise to an either outward or inward shift (with the size of the banana width) depending on the launch direction - outward for counter-passing electrons and inward for co-passing ones. In addition to collisions, the runaways experience a reaction force from the emission of synchrotron radiation. Although this does not change the particle positions much, because the energy loss is very small [11], it is nevertheless retained for purposes of completeness.

The simulations show that the magnetic perturbation of the DED scatters the particles radially. This happens even when collisions and radiation is switched off. In the cases shown on figure 4, with collisions switched on, there is a visible increase in the scatter of the particles due to the DED. Comparing figure 4b with figure 4c and figure 4e with figure 4f shows that the magnitude of the DED-current is not too significant in the width of the radial spreading of the particles.

Since the net radial displacement caused by the passing-trapped transition depends on the particle direction, the counter-passing particles reach the edge stochastic zone much

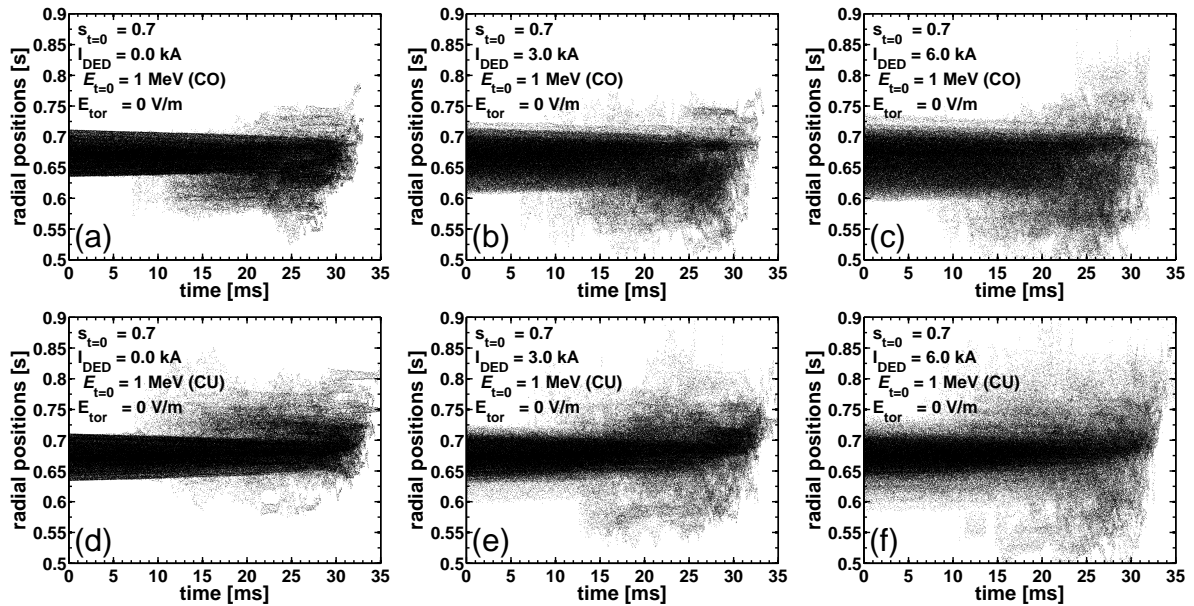


Figure 4: *Time dependence of the radial position of 100 electrons with initial energy 1 MeV launched at flux-surface $s = 0.7$ (a) $I_{DED} = 0$ kA, (b) $I_{DED} = 3$ kA, (c) $I_{DED} = 6$ kA, all co-passing, with initial pitch $v_{\parallel}/v = 1$ (TEXTOR case); (d)-(f) the same for counter-passing, with initial pitch $v_{\parallel}/v = -1$.*

faster than the co-passing particles. For this reason the co-passing (realistic) particles are less affected by the DED than the counter-passing ones. These results illustrate that including collisions in the simulation and using a collision operator that is valid for arbitrary energies is therefore a significant improvement over previous drift-only based simulations of the effect of RMP on runaway dynamics.

To be able to analyze the behavior of monoenergetic particles and the effect of collisions in the simulations presented above, the toroidal electric field was set to be zero. In this case, due to the collisions, the 1 MeV electrons launched at $s = 0.7$ are thermalized within 35 ms due to friction against thermal electrons. The background density plays a key role in the behavior of the low energy (e.g. ~ 1 MeV) runaway electrons. If we decrease the density by a factor of two, the thermalization time is doubled. If the particles are launched further in, for example at flux-surface $s = 0.5$, where the density is higher, most low energy particles are thermalized already after 20 ms. There is no notable difference between cases with and without DED if we investigate particle energy losses: the magnetic perturbation has practically no influence on the thermalization process.

If the toroidal electric field is assumed to be zero, too fast thermalization for the low-energy particles in the simulation can prevent possible orbit losses, leading to the underestimation of the DED induced drift orbit losses. As we have seen, the shrinkage of the confinement zone with increasing energy also plays an important role. However, to be able to analyze particle energy issues correctly, the accelerating electric field has to be taken into account. A simple estimate of the toroidal electric field during the disruption is [9]: $E_{\parallel} \simeq (L/2\pi R) \cdot dI/dt \simeq (\mu_0/2\pi) \cdot dI/dt$ where we have approximated the plasma inductance by $L \simeq \mu_0 R$. If we use the experimental value of $dI/dt \simeq 70$ MA/s [5] we arrive to $E_{\parallel} = 14$ V/m. For simulations with electric field this constant value was used, since the self-consistent computation of the accelerating force during runaway generation is non-trivial [16]. Collisions play a minor role compared with the electric field of this magnitude that

leads to a rapid acceleration of the runaways, preventing thermalization.

There is a maximum energy E that a runaway electron can gain in a tokamak disruption, since $dE/dt = -ev \cdot \mathbf{E} \leq -ec\partial A_{\parallel}/\partial t$ for any charged particle accelerated by an inductive electric field. In a tokamak $A_{\phi} = \psi\nabla\phi$, where $2\pi\psi$ is the poloidal magnetic flux, so the energy is limited by $E \leq ec\delta\psi/R$, where $\delta\psi$ is the change in the poloidal flux caused by the decay of the plasma current. If the aspect ratio is large and the cross section circular we have $d\psi/dr = rB/q(r)$, so on the axis (where the drop in ψ is the largest) $\delta\psi \leq B \int_0^a [r/q(r)]dr \lesssim Ba^2/4$ for a typical TEXTOR q-profile. Thus the maximum reachable energy is $E \leq eca^2B/4R \simeq 20$ MeV for the simulation parameters. If the initial 320 kA plasma current decays with $dI/dt \simeq 70$ MA/s, the current decay time is 4.6 ms, and the calculated $E_{\parallel} = 14$ V/m acting for 4.6 ms can accelerate a particle up to $\simeq 19.3$ MeV. This shows the consistency of the energy limit estimation. Simulations with a constant accelerating electric field show unrealistic results after $\simeq 4.6$ ms simulation time.

5. Runaway losses

In TEXTOR, the application of DED perturbation fields resulted in a significant decrease of the runaway population [5]. Interestingly, the current decay rate showed no dependence on the type of perturbation and its magnitude. However, in a few cases runaways were not suppressed even when the DED-current was higher than in other effective cases. In order to understand these experimental facts we have investigated the loss of runaway electrons as a function of time with respect to several parameters such as different DED currents, initial particle energies or positions. In the loss simulations we launched 100 monoenergetic particles parallel to the magnetic field. A particle is considered lost if it leaves the computational zone (LCFS).

Figure 5 shows the time-dependence of the loss fractions for two different initial energies, 10 and 30 MeV launched at the flux-surface $s=0.7$. For such high energies, a large fraction of the particles leave the confinement region due to immediate drift orbit losses within 45 nanoseconds. However, for those particles that remain inside the confinement region the further losses are less than 2%. The DED does not influence these immediate losses, and the curves are the same for every DED current. The curves are also the same with and without electric field. High energy immediate losses depend mainly on the particle energies: the immediate losses are caused by the shrinkage of the confinement zone.

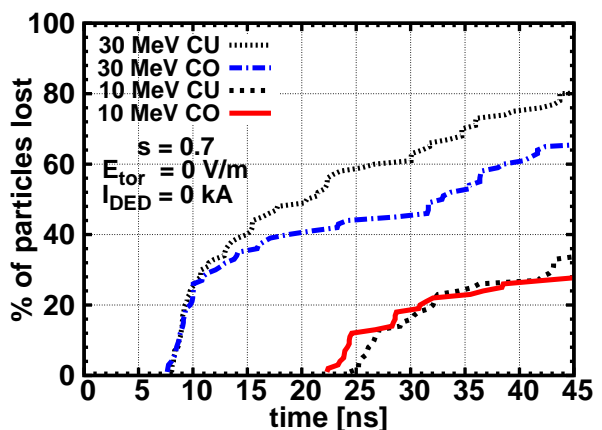


Figure 5: *Time dependence of immediate particle losses for 10 and 30 MeV, launched at $s=0.7$, both co- and counter-passing. All the particle losses occur before 45 ns (immediate losses). The magnetic perturbation or the electric field plays no role.*

Our simulations show that the electric field does not play a role in the immediate particle losses, but it does play a role in losses afterwards. In figure 6 the loss fractions are shown for 0 and 6 kA DED current in the case of 1, 10 and 30 MeV initial particle energies for co-

passing particles launched at $s=0.7$. For low energy particles the DED influences the onset time of the losses. There is a ~ 0.5 ms shift in the 1 MeV case. This shift may play a role in avalanche generation. It is interesting to note that for the 1 MeV electrons, both without DED and with a 6 kA DED-current, all the particles get lost within $\simeq 4$ ms. The time dependence of the losses of higher energy electrons (10 MeV and 30 MeV) is more interesting. As in the case for the 1 MeV electrons 85-90% of the particles get lost within 3.5 ms, but the remaining particles are confined for longer times, and interestingly the effect of DED can even increase the confinement time. This puzzling result is an artifact of the interplay of the monoenergetic distribution launched at $s=0.7$ and the spreading of the particles.

Regardless of DED, the particles launched at the same flux-surface have random banana orbit phases and hence get an instant spread dictated by the banana width. The banana width is larger for higher energy particles, and therefore higher energy particles moving inwards can penetrate much deeper in the plasma and thus kept confined for longer time before they finally get lost. The additional spreading due to DED may even increase the inward drift and consequently may then lead to an artificial confinement increase. This does not happen if the particles are launched in the plasma center, but in that case they do not reach the plasma boundary within the $\simeq 5$ ms lifetime of the accelerating electric field.

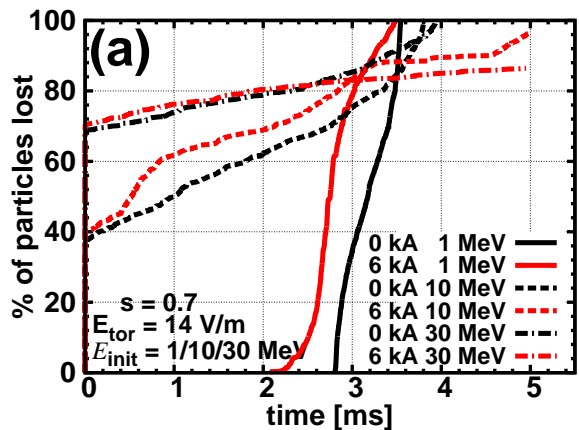


Figure 6: *Time dependence of particle losses with electric field, launched at $s=0.7$. 0 and 6 kA case with 1, 10 and 30 MeV initial energies. DED influences the long-term behaviour of particle losses.*

The detailed parameter scans carried out lead to some fundamental conclusions. The higher the energy of the particle, the lower the effect of the resonant perturbation on it. The higher the initial energy, the shorter is the onset time for particle losses - this is due to the fact that the losses mainly occur through the shrinkage of the confinement zone. However, the time between the first and last particle loss decreases with smaller initial energies. The reason for this is that the high energy particles reach the plasma edge faster, but are less sensitive to the magnetic perturbations.

The statistical significance of the simulations can be improved by increasing the number of particles. The standard deviation can be estimated with $\sigma(N) \simeq \sqrt{N}$ that is for 1000 particles $0 < \sigma < 32$. Our results show that further increasing the number of test particles does not influence the start- or endpoints, nor the slope of the loss rate curves. The only effect is that the lines are somewhat smoother, but the increase in the required CPU time is too large to motivate this small improvement.

5. Conclusions

We have studied the effect of perturbed magnetostatic fields on runaway electrons. In the simulations we have used a TEXTOR-like equilibrium and calculated the runaway drift orbits to study the losses for various runaway electron energies and magnetic perturbations. The calculations are done with the ANTS code extended for the purposes of this work to include synchrotron radiation losses and a collision operator valid for arbitrary

particle energy (but neglecting Bremsstrahlung). The effect of the collision operator was illustrated in simulations without an accelerating electric field.

We found that runaway electrons in the core of the plasma are likely to be well confined. Particles in the plasma center do not get lost either during the lifetime of the toroidal electric field, or in the longer time interval without significant toroidal electric field that follows. For low-energy ($\simeq 1$ MeV) particles closer to the boundary the onset time of the losses is dependent on the amplitude of the magnetic perturbation. The runaway current damping rate is however insensitive to the magnetic perturbation level. As expected, the energies of the particles are not affected by the magnetic perturbation. Synchrotron radiation emission does not contribute much to the losses, mainly due to the fact that the time-scale of these losses is much longer than the runaway loss time.

Our results indicate that the loss of high-energy ($\gtrsim 10$ MeV) runaways in the simulation is mostly due to the fact that their orbits are wide, which allows them to intersect the wall. The loss is dominated by the shrinkage of the confinement region, which is independent of the DED current. We have illustrated this in particle Poincaré plots, where the shrinkage is clearly visible for high energies. Note that this only stands for particles launched close to the plasma periphery. We expect the experimental results to be reproducible only by more complex simulations including the temporal evolution of the magnetic structure and the indirect effects of the RMP on runaway electron generation and loss processes.

Acknowledgements

This work was funded by the European Communities under Association Contract between EURATOM, *Vetenskapsrådet*, HAS and Germany. The views and opinions expressed herein do not necessarily reflect those of the European Commission. The authors would like to thank M. Lehnen and O. Schmitz for providing the TEXTOR data.

References

- [1] P. HELANDER ET AL. *Plasma Physics and Controlled Fusion*, **44** (12B):B247 (2002).
- [2] R. YOSHINO ET AL. *Nuclear Fusion*, **40** (7):1293 (2000).
- [3] K. FINKEN ET AL. *Nuclear Fusion*, **46** (4):S139 (2006).
- [4] K. FINKEN ET AL. *Nuclear Fusion*, **47** (2):91 (2007).
- [5] M. LEHNEN ET AL. *Phys. Rev. Lett.*, **100** (25):255003 (2008).
- [6] M. LEHNEN ET AL. *Journal of Nuclear Materials*, **390-391**:740 (2009).
- [7] P. GHENDRIH ET AL. *Plasma Physics and Controlled Fusion*, **38** (10):1653 (1996).
- [8] V. RICCARDO ET AL. In *Europhysics Conference Abstracts*, vol. 34 (2010).
- [9] P. HELANDER ET AL. *Physics of Plasmas*, **7** (10):4106 (2000).
- [10] M. DREVLAK. In *Europhysics Conference Abstracts*, vol. 33E, P-4.211 (2009).
- [11] G. PAPP ET AL. *Nuclear Fusion* (2010). Submitted.
- [12] S. P. HIRSHMAN ET AL. *Computer Physics Communications*, **43** (1):143 (1986).
- [13] S. ABDULLAEV ET AL. *Nuclear Fusion*, **43** (5):299 (2003).
- [14] K. FINKEN ET AL. *The structure of magnetic field in the TEXTOR-DED*. Grafische Medien, Forschungszentrum Jülich GmbH, Jülich (2005).
- [15] M. F. HEYN ET AL. *Nucl. Fusion*, **48** (1):0240052 (2008).
- [16] L.-G. ERIKSSON ET AL. *Phys. Rev. Lett.*, **92** (20):205004 (2004).